Electrochimica Acta 204 (2016) 146–153

Contents lists available at ScienceDirect

Electrochimica Acta

journal homepage: www.elsevier.com/locate/electacta

Supercapacitive characteristics of carbon-based graphene composites

P. Bharathidasan[a], Dong-Won Kim[b], S. Devaraj[a], S.R. Sivakkumar[a,*]

[a] School of Chemical and Biotechnology, SASTRA University, Thanjavur 613 401, India
[b] Department of Chemical Engineering, Hanyang University, Seoul 133-791, Republic of Korea

ARTICLE INFO

Article history:
Received 22 December 2015
Received in revised form 25 March 2016
Accepted 12 April 2016
Available online 13 April 2016

Keywords:
Graphene
Reduced graphene oxide
Graphene composite
Supercapacitor
Electrochemical capacitor

ABSTRACT

Graphene, also referred as reduced graphene oxide (RGO) is prepared by chemical exfoliation method, which delivers specific capacitance of 77 and 40 F g^{-1} at 0.1 and 1.0 A g^{-1}, respectively in aqueous electrolyte. In order to improve the specific capacitance and high power performance of RGO, composites of RGO are prepared with various carbonaceous 'spacer' materials such as acetylene black (AB), activated carbon (AC), multi-walled carbon nanotube (CNT) and carbon derived from polyaniline (C-PANI). Composites of RGO with spacer materials such as AB, AC and CNT is prepared by mechanically mixing RGO with the spacer materials; whereas, RGO composite with C-PANI is prepared by *in situ* method. These two different preparation methodologies are adopted to realise its effect on the physical and electrochemical characteristics of the composites. Morphological, X-ray diffraction and Raman data confirm the formation of mixture of few and multi-layered RGO stacks. Surface area analysis and morphological data show that the composite prepared by *in situ* method is beneficial in achieving higher specific surface area and improved mesoporosity. Specific capacitance of RGO and its composites obtained at 0.1 A g^{-1} decreased in the order: RGO/C-PANI (165 F g^{-1}) > RGO/AC (121 F g^{-1}) > RGO/AB (107 F g^{-1}) > RGO/CNT (95 F g^{-1}) > pristine RGO (77 F g^{-1}). Capacitance retention of RGO and its composite electrodes (in percentage) at 1.0 A g^{-1}, in comparison with the value obtained at 0.1 A g^{-1} decreased in the order: RGO/AB (84%) > RGO/CNT (75%) > RGO/AC (71%) > RGO/C-PANI (64%) > pristine RGO (52%).

1. Introduction

Currently, research work on graphene and its composites for supercapacitor applications is intensely pursued world-wide. Numerous research articles and reviews have been published on this subject [1–8]. For supercapacitor applications, what are attractive with graphene as electrode material are its superior electrical conductivity (higher than copper, > 10^9 S cm^{-1}), high specific surface area (2600 m^2 g^{-1}) and its flat sheet-like structure. In commercial supercapacitors, AC is the widely used electrode active material. While AC has decent electrical conductivity (1.0–5.0 S cm^{-1}), it is much lower than the conductivity of graphene. AC with high specific surface area (~2500 m^2 g^{-1}) can also prepared, but such a high surface area is achieved only with the development of lots of micropores on the AC surface. Although the micropores contribute for the total surface area, charge storage in 'smaller' micropores is rather difficult and often adversely affects the power characterisistics of AC electrodes. Because of the flat sheet-like structure of graphene and its high surface area, when used as electrode material in supercapacitors, high power capability and high specific capacitance (theoretical specific capacitance: 550 F g^{-1}) is expected. Above all, the precursor of graphene, graphite (Gr), being low cost and environmentally friendly is another attractive feature of graphene.

Graphene is prepared from graphite by several methods such as epitaxial and chemical vapour deposition growth [9,10], micro-mechanical exfoliation of graphite [11], exfoliation of graphite in organic solvents [12], arc-discharge synthesis of multi-layered graphene; [13] and chemical exfoliation methods [14,15]. Among these methods, chemical exfoliation method is viable for large scale production and is widely used in the literature. One of the challenges with graphene preparation is, keeping individual graphene sheets away from restacking, once after its preparation. Restacking of graphene sheets happens due to π- π attraction. Once restacking happens, the surface area available for charge storage and the electrical conductivity decreases. In order to prevent restacking of graphene, several studies have been devoted for the preparation of graphene composites [16–27]. In these studies, graphene composites have been prepared using various 'spacer' materials such as carbons, metal oxides and polymers.

* Corresponding author. Tel.: +91 4362 264101; fax: +91 4362 264120.
E-mail addresses: srsivakkumar@yahoo.com, srsivakkumar@scbt.sastra.edu (S.R. Sivakkumar).

http://dx.doi.org/10.1016/j.electacta.2016.04.064
0013-4686/

These spacer materials reside in-between graphene sheets, thereby prevent restacking and generate sufficient space for the entry/exit of counter ions for charge storage/delivery. Specific capacitance values reported for graphene and its composites prepared by chemical exfoliation method are in the range of 30–365 F g^{-1} [16–27]. It can be deduced from these reports that the specific capacitance contribution by the graphene alone in the composites is only in the range of 30–150 F/g and the remaining higher capacitance obtained is due to the redox contribution by the metal oxides and polymers. Despite the specific capacitance values of pristine graphene are found to be improved in the composites (30–150 F/g), they are still far less than the theoretical value (theoretical value: 550 F/g); indicating that the effective separation of graphene sheets by spacer materials in the composites are yet to be improved and the complete separation remains a challenge. The wide variation in the specific capacitance values of graphene (itself) reported in the literature is due to the difference in the number of graphene layers that exist as a stack in each material. As the number of layers in a stack decreases, specific capacitance increases and *vice versa*. Since graphene exist intrinsically as multilayer due to π- π attraction, it is commonly referred as reduced graphene oxide (RGO) in the literature.

In the present study, we prepared RGO by chemical exfoliation method as it is viable for large scale production. We also prepared composites of RGO with carbonaceous materials such as AB, AC, CNT and C-PANI. Composites of RGO were prepared by two different methods: (i) mechanical mixing of RGO with spacer materials such as AB or AC or CNT and (ii) *in situ* preparation of RGO composite with C-PANI. These two different preparation methods were chosen to understand its effect on the prevention of restacking of graphene and consequently its charge storage capacitance.

2. Experimental

All the chemicals used in this study were purchased from Aldrich and Merck chemicals. Graphite oxide was prepared by modified Hummers' method [15,28]. After removing the reaction by-products, graphite oxide obtained was sonicated using PCI Analytics ultrasonic bath for at least 2 hours to prepare graphene oxide (GO). Finally, GO suspension was reduced by using hydrazine to get reduced graphene oxide (RGO) [29,30]. It should be mentioned that in some studies, in order to prepare RGO stacks having few-layered graphene sheets, the GO suspension was centrifuged at different rpm and only the residue obtained at very high rpm (around 16000) were utilised (the residue obtained at low rpm were discarded as it contains stacks of multi-layered graphene). However, in the present study, we have not centrifuged GO suspension to separate GO stacks having different number of graphene sheets. The yield of RGO in our case was as high as 75%.

Composites of RGO with AB or AC or CNT were prepared by mechanically mixing RGO (83 wt.%) with AB or AC or CNT (10 wt.%) (The remaining 7 wt.% was binder material as mentioned below) using a mortar and pestle. Composite of RGO with C-PANI was prepared as follows: 2.0 g of GO was first dispersed in 1 litre of 1.0 M HCl by sonicating the solution for two and half hours. Then 0.2 ml of aniline monomer was mixed with the GO suspension. This mixture was sonicated for another 1 hour to facilitate adsorption of monomer on the GO surfaces. Thereafter, ammonium persulfate solution (11.41 g in 250 ml water) was added slowly into the GO/aniline mixture under ice-cold condition with constant stirring. After the addition of ammonium persulfate solution was over, stirring was continued for 12 hours also under ice-cold condition. The GO/PANI composite formed was then washed with water, filtered, dried and weighed. The total weight of GO/PANI was found to be 2.258 g. From this, only 2.0 g of composite was carbonised by heating at a rate of 5° C min^{-1} to 900 ° C under flowing N_2. The sample was kept at the maximum temperature (900 ° C) for 1 hour and allowed to cool naturally to room temperature, also under flowing N_2. The weight of carbonised sample was found to be 1.0381 g. In a control experiment, weighed quantity of GO and PANI were heated independently to 900 ° C under flowing N_2 and held at the maximum temperature for 1 hour and cooled to room temperature under flowing N_2 and the weight of the samples was measured. From this data, the ratio of RGO and carbon derived from PANI (C-PANI) present in 1.0381 g of RGO/C-PANI composite was determined to be 90:10 wt.%.

Surface morphologies of RGO and its composites were analysed by using scanning electron microscope (SEM, JEOL JSM-6330F) and transmission electron microscope (TEM, JEOL JEM 2100F). Powder X-ray diffraction (XRD) analysis of samples was made by using X-ray diffractometer (D8 Focus, Bruker AXS, Germany) and Raman spectroscopic analysis of samples was performed by using Dongwoo optron, MonoRa 780i spectrometer. A green laser

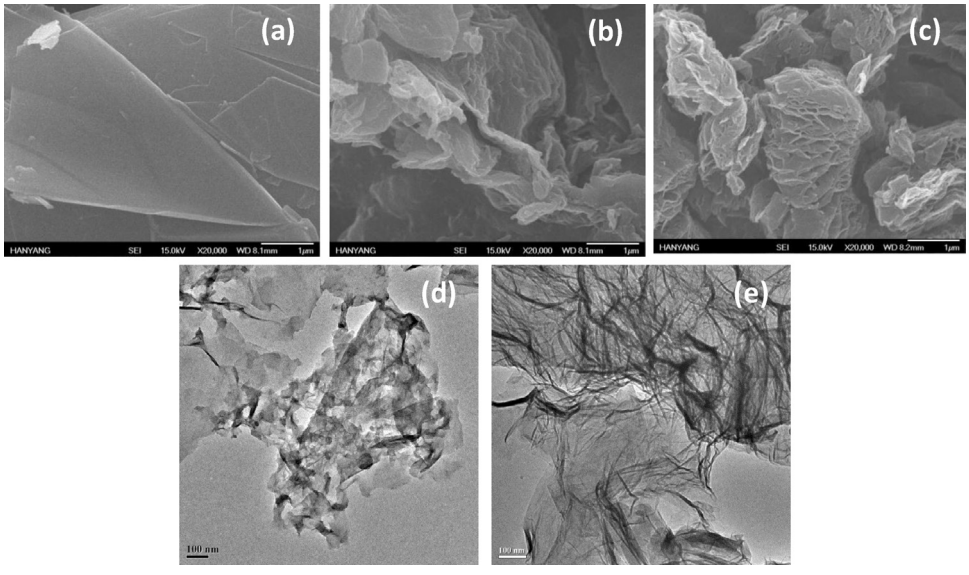

Fig. 1. SEM images of (a) graphite, (b) RGO, (c) RGO/C-PANI and TEM images of (d) RGO and (e) RGO/C-PANI.

(532 nm) having 2.3 mW power was used as the excitation source in Raman spectra. Brunauer, Emmett and Teller (BET) surface area measurements were made by using the surface area analyser, micromeritics ASAP 2020.

In order to prepare coated electrodes of RGO and its composite with AB, AC, CNT and C-PANI, active materials (93 wt.%) (85 wt.% for RGO/C-PANI only) were mixed with polyvinylidene fluoride (PVdF) binder (7 wt.%) (15 wt.% for RGO/C-PANI only) and a slurry was prepared using dimethyl formamide (DMF), which was then coated onto stainless steel foils to an area of 1 cm^2. Approximate loading of active materials was 2 mg cm^{-2}. A 0.25 M H_2SO_4 was chosen as the electrolyte. Biologic potentiostat (SP-200) was used for the electrochemical characterisation of the electrode materials. Stainless steel electrodes coated with the active materials were used as the working electrode. Pt foil and Ag/AgCl electrodes served as counter and reference electrodes, respectively.

3. Results and discussion

3.1. Physical characterisation

Morphologies of Gr, RGO and RGO/C-PANI are shown in Fig. 1. The Gr flakes purchased from Aldrich chemicals display flake-like morphology. Morphology of RGO recorded at the same magnification as that of Gr shows exfoliated graphene sheets; however, there is no complete exfoliation observed. RGO/C-PANI displays higher

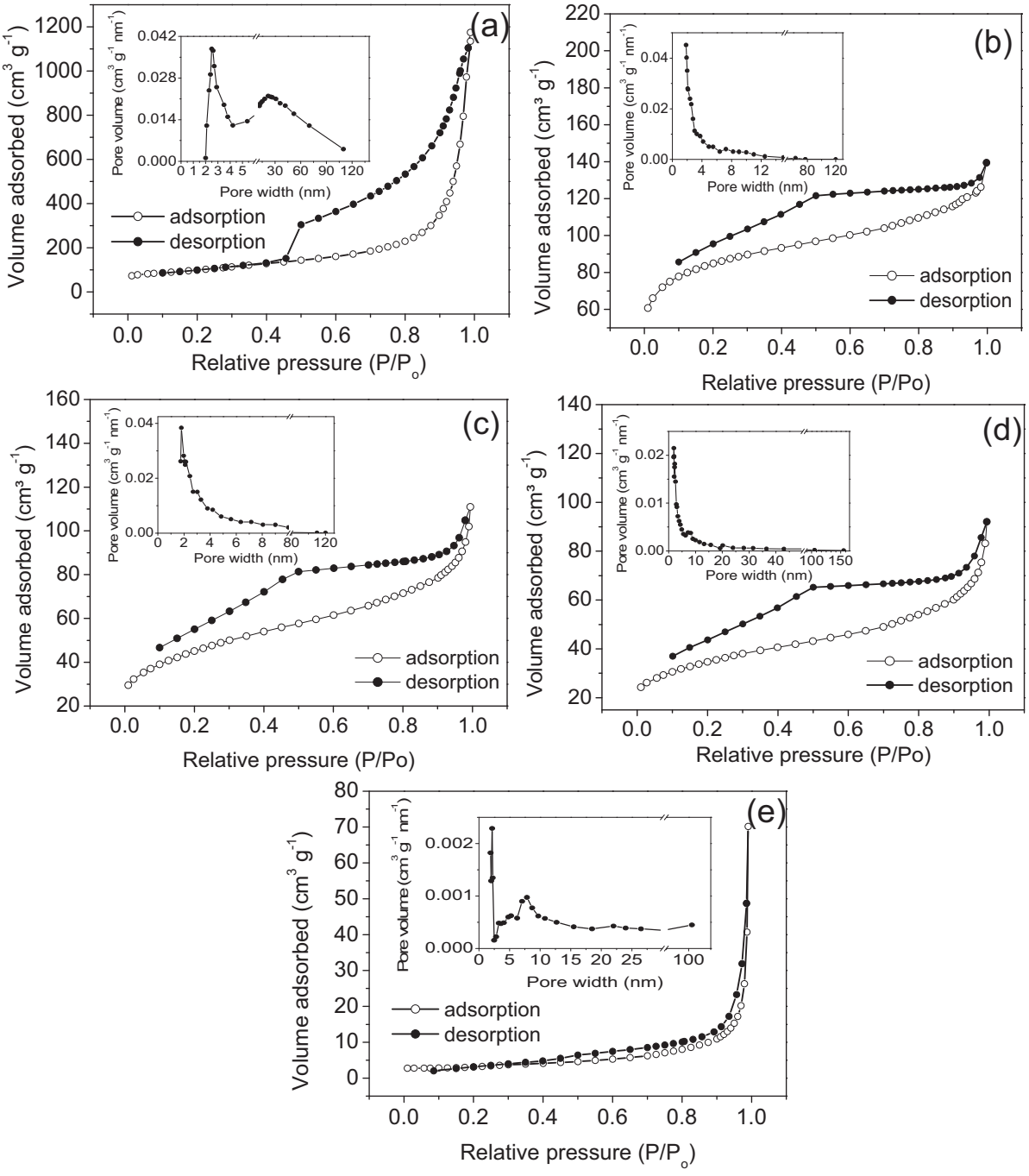

Fig. 2. Nitrogen adsorption and desorption isotherms of (a) RGO/C-PANI, (b) RGO/AC, (c) RGO/AB, (d) RGO/CNT and (e) RGO. Inset: BJH pore size distribution.

degree of exfoliated graphene sheets compared to RGO. Presence of carbon derived from PANI in RGO/C-PANI composite appear to act as a spacer and inhibit restacking of graphene layers, which could be one of the reasons for the higher degree of exfoliation seen in RGO/C-PANI. In addition, in order to prepare RGO, GO was chemically reduced by hydrazine; whereas, for the preparation of RGO/C-PANI, no chemical reduction was employed, instead, GO/PANI composite was heat-treated at 900 °C. Such a high temperature usually carbonises PANI and reduces most of the functional groups present in the GO. This difference in the synthetic procedure could also be one of the reasons for the higher degree of exfoliation seen in RGO/C-PANI (high temperature is known to induce exfoliation of graphite [31,32]). Moreover, presence of very thin graphene sheets are also seen in the TEM images of RGO (Fig. 1d) and RGO/C-PANI (Fig. 1e) indicating that these materials composed of mixture of (few and multi-layered) graphene stacks. Hairline-like streaks seen in RGO/C-PANI (Fig. 1e) are believed to be the carbon derived from PANI and/or highly wrinkled RGO sheets.

Nitrogen adsorption-desorption isotherms of RGO and RGO/C-PANI samples are shown in Fig. 2. The isotherms exhibit type IV adsorption isotherm with sharp capillary condensation step and a type 2 hysteresis loop, which is characteristic of mesoporous material [33]. Multi-point BET surface area measured for RGO/C-PANI, RGO/AC, RGO/AB, RGO/CNT and RGO showed specific surface area of 346, 274, 155, 117 and 11 $m^2 g^{-1}$, and that of total mesopore volumes were measured to be 1.78, 0.12, 0.14, 0.11 and 0.10 $cm^3 g^{-1}$, respectively. Barrett-Joyner-Halenda (BJH) pore size distribution obtained from adsorption branch of the isotherms (shown as inset in Fig. 2) show that RGO/C-PANI, RGO/AC, RGO/AB, RGO/CNT and RGO has mesopores with pore sizes around 2 & 25, 7, 2, 2 & 8 and 2 & 7 nm, respectively. The large size mesopores present in the composite is expected to favour smooth entry/exit of counter ions during charge/discharge. The BET surface area values of RGO and RGO/C-PANI correlate very well with their morphological data and indicate that as these values are far less than the theoretical surface area value of graphene, exfoliation of graphene sheets were incomplete in both the materials.

Power XRD patterns obtained for Gr, RGO and RGO/C-PANI are shown in Fig. 3. The (002) ($2\theta = 26.4$) and (004) ($2\theta = 54.5$) peaks, which are the two strongest characteristic peaks in the XRD pattern of natural graphite, represent perpendicular direction (c-axis) to the graphite hexagonal planes [34]. These two peaks are almost vanished in RGO and RGO/C-PANI, meaning that the orderly stacking structure of graphite is destroyed in the latter materials.

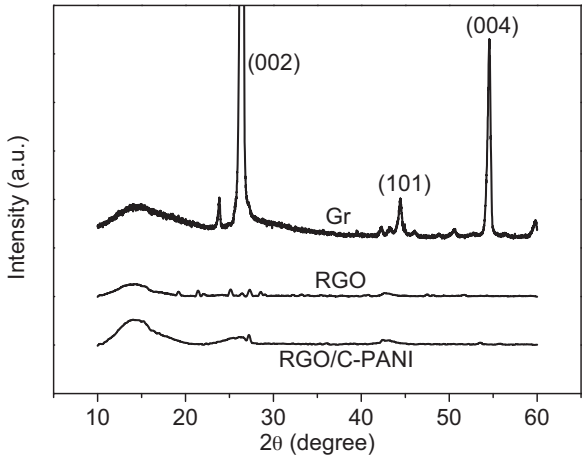

Fig. 3. Powder XRD pattern of graphite, RGO and RGO/C-PANI.

Raman spectra recorded for Gr, RGO and RGO/C-PANI are shown in Fig. 4. Both RGO and RGO/C-PANI display G band (1580 cm^{-1}) and D band (1350 cm^{-1}), which are characteristic Raman spectrum of graphene [35,36]. The G band denotes graphitic band and the D band denotes disordered or defective band. Raman spectrum of graphite shows only G band and the intensity of D band is negligibly small. Any physical or chemical treatment which causes defects or disorder in pristine graphite will result in the appearance of D band. However, the 2D band (2716 cm^{-1}) appearing for both graphite and RGO samples do not refer disorder, but appears in the spectrum due to the first overtone of D band. The intensity ratio of 2D and G band is used to identify single layer graphene. For a single layered graphene, I_{2D}/I_G is ~2.0. It has been reported that as the number of graphene layers increases in a stack, the intensity of G band increases but the intensity of 2D band decreases and broadens [35–37]. In order to estimate the I_{2D}/I_G ratio for the RGO and RGO/C-PANI composite, the G and 2D bands in the Raman spectra of these materials are deconvoluted (Fig. 4b-4e) as per the reported literature [35–38]. The I_{2D}/I_G value obtained for the RGO is 0.347 and that for the RGO/C-PANI is 0.753. These results indicate both the materials contain stacks of multilayered graphene sheets (more than 5 layers [35]) and the number of graphene sheets in the stacks of RGO/C-PANI is comparatively less than RGO, which is attributed to the effect of C-PANI in preventing the graphene sheet restacking in the composite. However, the exact number of graphene layers present in the RGO and its composite from the ratio of their I_{2D}/I_G value may not be deduced and any value lower than 2 is only indicative of the presence of multi-layered graphene. As such, for the bulk graphite, the number of graphene layers cannot be deduced from its Raman spectrum and therefore the calculation of I_{2D}/I_G for the bulk graphite is of no significance [35].

3.2. Electrochemical characterisation

Cyclic voltammograms of RGO and RGO/C-PANI electrodes recorded at two different scan rates are shown in Fig. 5. In the same figure, cyclic voltammograms of composites of RGO with AB, AC and CNT are also shown. As mentioned in the earlier sections, while RGO/C-PANI was prepared by *in situ* method, the other composites were prepared by mechanical mixing of RGO with the spacer materials. Preparation of the latter composites by *in situ* method was not possible as the wettability of the spacer materials (AB, AC and CNT) was very poor in aqueous medium.

At the scan rate of 2 mV s^{-1}, all the five electrodes show nearly rectangular voltammogram, characteristic of supercapacitors. However, some deviation from rectangular shape seen around 0.2 V on either side of the scan is most likely due to the redox reaction of residual functional groups present in RGO materials. Among all the voltammograms, specific capacitance values of RGO/C-PANI is the highest, pristine RGO is the lowest and the values of other composite materials are in-between the above two values. Effect of spacer materials in improving the charge storage capacitance of RGO is obvious from these results. Moreover, the highest specific capacitance value displayed by the RGO/C-PANI is believed to be due to the effective separation of RGO by the C-PANI, as this composite was prepared by *in situ* method. From the control experiments, specific capacitance of AB and CNT were estimated to be less than 1.0 F g^{-1}; whereas that of AC was around 147 F g^{-1}. For the specific capacitance calculation, weights of RGO and spacer materials are considered.

At 50 mV s^{-1}, all the five electrodes display decreased specific capacitance and some resistive behaviour in the voltammogram. Therefore, the voltammograms are somewhat distorted from the

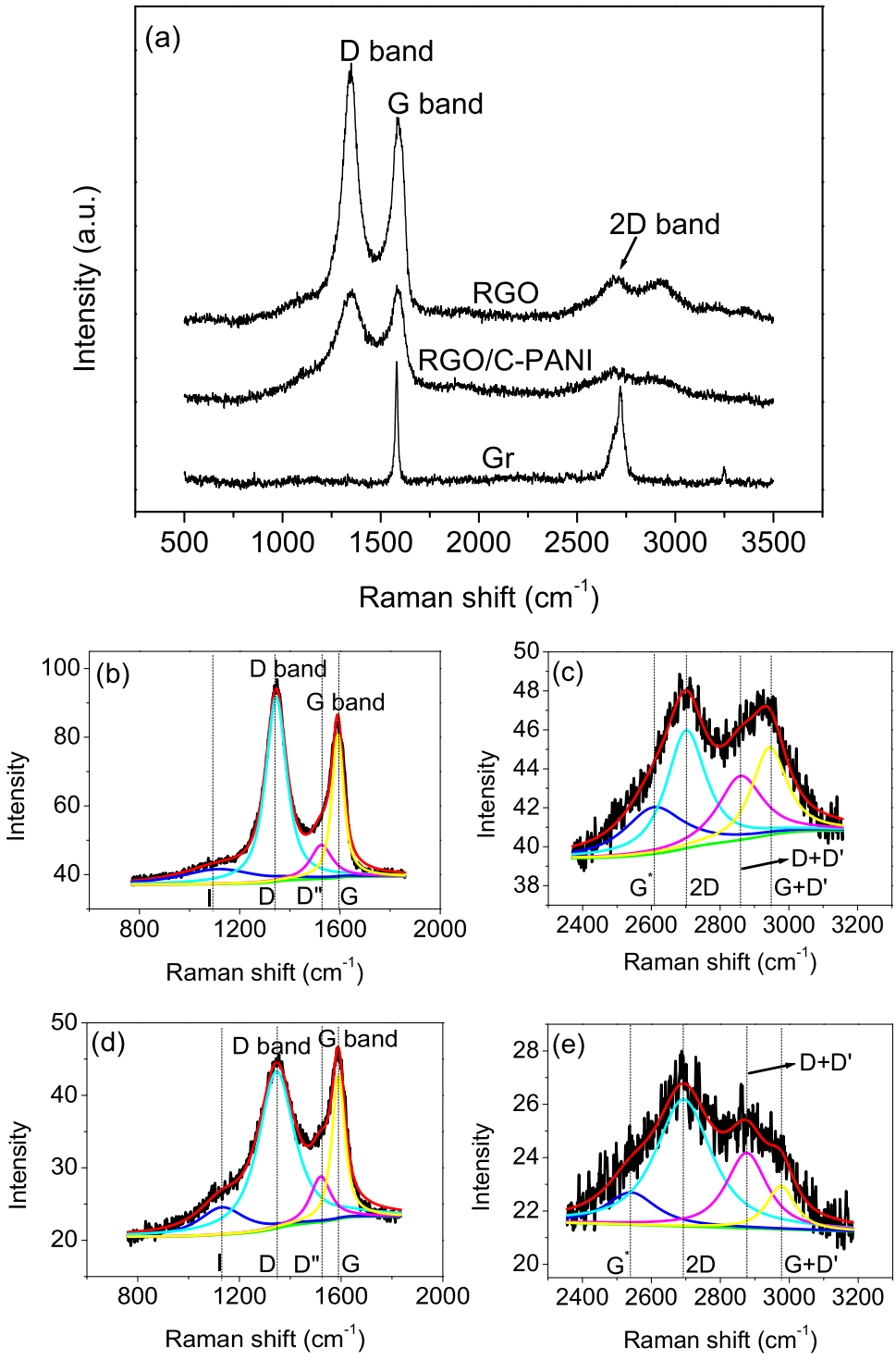

Fig. 4. Raman spectra of (a) graphite, RGO and RGO/C-PANI, (b) & (c) deconvoluted Raman spectrum of RGO and (d) & (e) deconvoluted Raman spectrum of RGO/C-PANI.

rectangular shape. Whilst the graphene has excellent electrical conductivity, the material prepared by using Hummers' method and subsequent reduction by hydrazine or annealing at high temperature is shown to contain some defects and residual functional groups [30] (which are also evident from Raman and cyclic voltammetric data). The presence of defects and functional groups has been said to decrease the electrical conductivity of graphene. Moreover, the RGO prepared in this study contains multi-layered graphene, whose electrical conductivity is also expected to be less than single layered graphene. These are presumed to be the reasons for the relatively poor performance of RGO and its composite electrodes at high scan rate.

Chronopotentiograms recorded at two different current densities for the RGO and its composite electrodes are shown in Fig. 6. At both the current densities, all the five electrodes exhibit linear charge/discharge profile with a minimal iR drop. RGO/C-PANI electrode takes longer time to fully charge/discharge and the pristine RGO takes the shortest time while the time taken by other

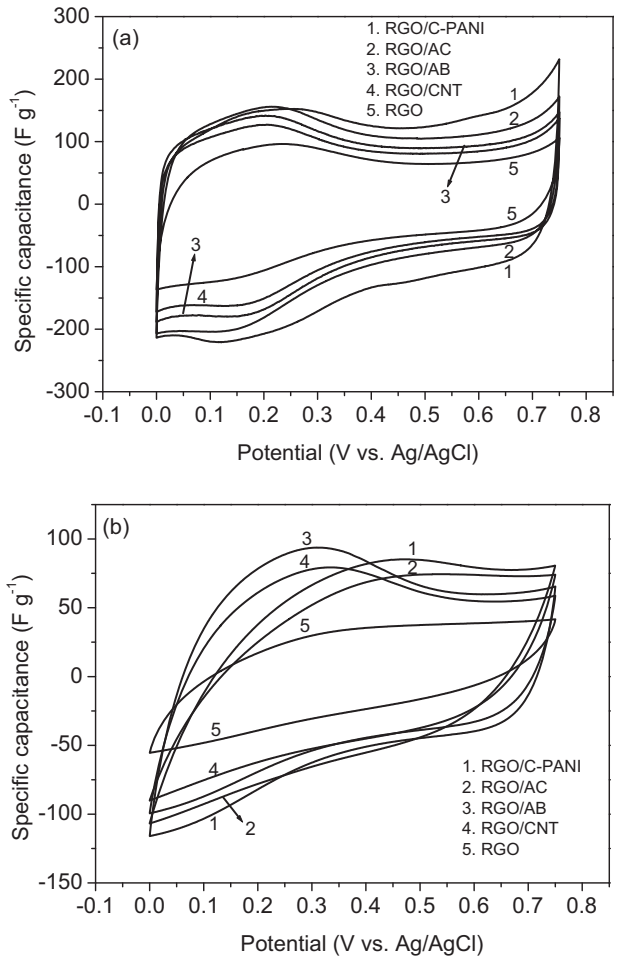

Fig. 5. Cyclic voltammograms of RGO and its composite electrodes recorded at (a) 2 mV s^{-1} and (b) 50 mV s^{-1}.

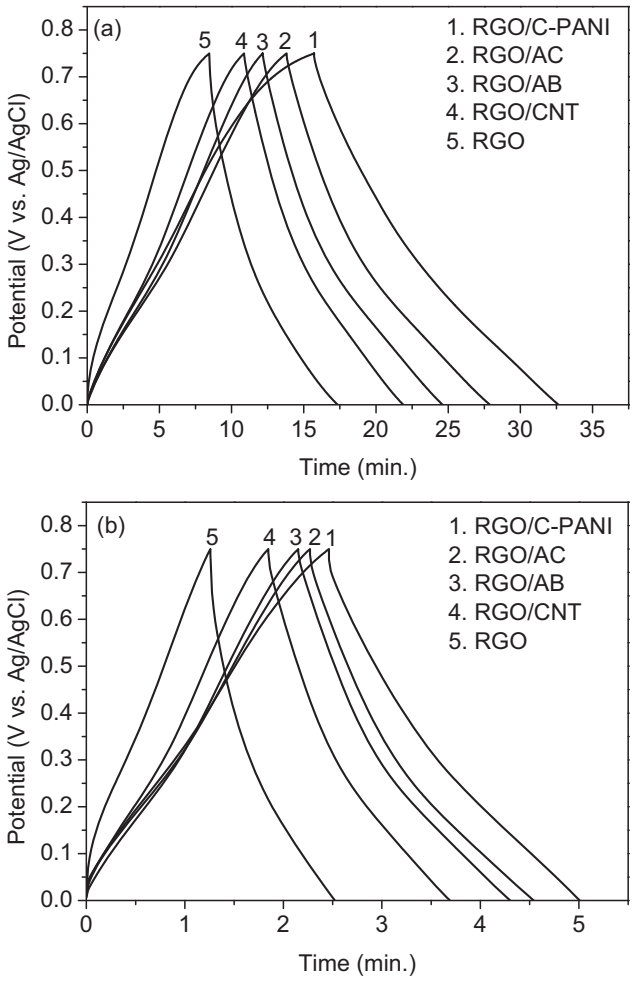

Fig. 6. Chronopotentiograms of RGO and its composite electrodes recorded at a current density of (a) 0.1 A g^{-1} and (b) 0.5 A g^{-1}.

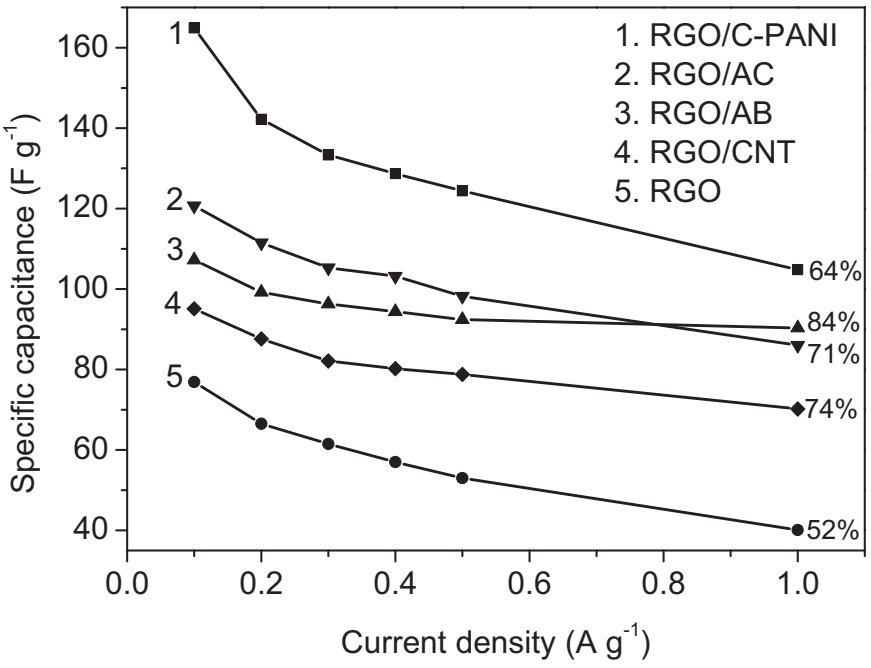

Fig. 7. Effect of charge/discharge current density on the specific capacitance of RGO and its composite electrodes.

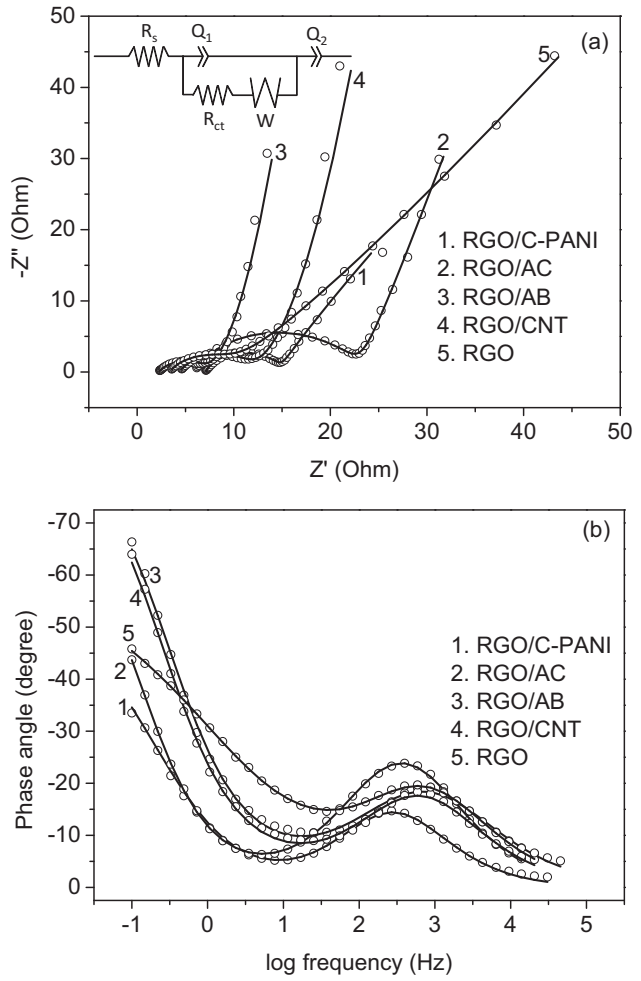

Fig. 8. (a) Nyquist plot of RGO and its composite electrodes recorded at an applied DC potential of 0.4 V vs. Ag/AgCl. Applied AC potential: 10 mV; Frequency range: 100 kHz to 100 mHz. Raw data are shown as open circles and the fitted data are shown as solid lines. Inset: Equivalent circuit (R_s – solution resistance, R_{ct} – charge transfer resistance, W – Warburg resistance and Q_1 & Q_2–constant phase elements) and (b) Bode plots of RGO and its composite electrodes recorded at the above conditions.

composite electrodes are in-between the above two electrodes, which corresponds to their specific capacitance values.

Specific capacitance values of RGO and its composite electrodes computed at various applied current densities are presented in Fig. 7. Specific capacitance values were calculated from the discharge curves. At each applied current density, the charge current density was the same as that of the discharge current density. For the applied current density of 0.1 A g^{-1}, specific capacitance values decreased in the order: RGO/C-PANI (165 F g^{-1}) > RGO/AC (121 F g^{-1}) > RGO/AB (107 F g^{-1}) > RGO/CNT (95 F g^{-1}) > pristine RGO (77 F g^{-1}). The highest specific capacitance displayed by the RGO/C-PANI is believed to be due to its relatively high BET surface area (346 m^2 g^{-1}) and high mesopore volume (1.78 cm^3 g^{-1}). However, the RGO/AB shows the highest capacitance retention at 1.0 A g^{-1} (retains 84% of its capacitance obtained at 0.1 A g^{-1}). Specific capacitance retention for both RGO/AC and RGO/CNT are similar at 1.0 A/g. Pristine RGO has the lowest capacitance retention (at 1.0 A g^{-1}, retains 52% of capacitance obtained at 0.1 A g^{-1}). It should be highlighted that RGO/C-PANI required 15 wt.% of polymeric binder unlike other electrode materials which required only 7 wt.% of binder to achieve good adherent coating on the current collector. The higher percentage of binder material used in the case of RGO/C-PANI electrode is also thought to be responsible for the relatively poor capacitance retention at higher current densities. By optimising the coating procedure, further improvement in performance of RGO/C-PANI electrode is expected. It was also found that the sum of specific capacitance values of RGO and spacer materials (AB or AC or CNT or C-PANI) was less than the specific capacitance values of their corresponding composites. This indicates the existence of possible synergistic effect from RGO and spacer materials in the composite electrodes.

Table 1
Fitting results of the Nyquist and Bode plots using the equivalent circuit.

Electrode	Solution resistance (R_s) (Ohm)	Charge transfer resistance (R_{ct}) (Ohm)	Phase angle (degree) @ 100 mHz
RGO/C-PANI	7.11	8.34	−33.5
RGO/AC	5.86	17.03	−43.7
RGO/AB	2.22	5.09	−66.3
RGO/CNT	4.37	7.67	−64.0
RGO	3.36	6.91	−45.8

In the case of RGO prepared by chemical exfoliation method, in the literature, in order to obtain higher capacitance, generally multi-layered GO are separated out from the few-layered GO by means of centrifugation, performed at different rpm. In this way, it is possible to prepare RGO containing few-layered graphene that will deliver high specific capacitance, but the yield of RGO will be generally low in this case. In the present study, we have not used centrifugation to separate different fractions of GO. In fact, except in the case of RGO/C-PANI, we have not separated GO from its solution and directly reduced GO by hydrazine after removing the reaction by-products. Hence, the yield of RGO in the present study was as high as 75%.

AC Impedance spectra recorded for all the five electrodes are shown in Fig. 8. The impedance data have also been fitted. Equivalent circuit pertinent to the fitted curves is also given in Fig. 8(a). The solution (R_s) and charge-transfer resistances (R_{ct}) obtained from the fitted data for all the five electrodes are given in the Table 1. Bode plot obtained for the impedance measurement of all the RGO and its composite electrodes are shown in Fig. 8(b). The lowest frequency phase angle obtained for all the electrodes are also mentioned in the Table 1. The lowest R_{ct} and the highest phase angle obtained for the RGO/AB electrode is presumed to be reason for its best capacitance retention at higher current values among the five electrodes studied (Fig. 7). RGO/AC showed highest R_{ct} probably due to the presence of micropores present in AC, where the rate at which the counter ions entry into the small sized pores were restricted. The relatively highest value of R_s and lowest phase angle displayed by the RGO/C-PANI electrode is presumed to be due to the presence of relatively high amount of binder material in the electrode (15 *vs.* 7 wt.% used for making other electrodes).

4. Conclusions

RGO is prepared by chemical exfoliation method and the yield is as high as 75%. Specific capacitance of RGO and its composites obtained at 0.1 A g^{-1} decreased in the order: RGO/C-PANI (165 F g^{-1}) > RGO/AC (121 F g^{-1}) > RGO/AB (107 F g^{-1}) > RGO/CNT (95 F g^{-1}) > pristine RGO (77 F g^{-1}). The higher specific capacitance value obtained for RGO/C-PANI show that the *in situ* method employed for its preparation efficiently prevents graphene restacking. Capacitance retention of RGO and its composite electrodes (in percentage) at 1.0 A g^{-1}, in comparison with the value obtained at 0.1 A g^{-1} decreased in the order: RGO/AB (84%) > RGO/CNT (75%) > RGO/AC (71%) > RGO/C-PANI (64%) > pristine RGO (52%). The specific capacitance values obtained are far

less than the theoretical capacitance of graphene (theoretical value: 550 F g^{-1}). So, it is presumed that the extent of oxidation of graphite during the preparation of GO is not very efficient. Therefore, in order to prepare RGO at a large scale with high yield, procedure for more efficient oxidation of graphite needs to be devised.

Acknowledgments

S.R.S. gratefully acknowledges Department of Science and Technology (DST), India for financial support through Fast Track Scheme for Young Scientists (Grant No.: SB/FT/CS-70/2012). This work was partly supported by the Industrial Promotion Program of Economic Cooperation Area of MOTIE/KIAT [R0004005].

References

[1] Y. Huang, J. Liang, Y. Chen, An overview of the applications of graphene-based materials in supercapacitors, Small 8 (2012) 1805–1834.
[2] J. Zhang, X.S. Zhao, On the configuration of supercapacitors for maximizing electrochemical performance, ChemSusChem 5 (2012) 818–841.
[3] M.D. Stoller, S. Park, Y. Zhu, J. An, R.S. Ruoff, Graphene-based ultracapacitors, Nano lett. 8 (2008) 3498–3502.
[4] M. Pumera, Graphene-based nanomaterials for energy storage, Energy Environ. Sci. 4 (2011) 668–674.
[5] Y.B. Tan, J.M. Lee, Graphene for supercapacitor applications, J. Mater. Chem. A 1 (2013) 14814–14843.
[6] D. Chen, L. Tang, J. Li, Graphene-based materials in electrochemistry, Chem. Soc. Rev. 39 (2010) 3157–3180.
[7] R.R. Salunkhe, Y.H. Lee, K.H. Chang, J.M. Li, P. Simon, J. Tang, N.L. Torad, C.C. Hu, Y. Yamauchi, Nanoarchitectured graphene-based supercapacitors for next-generation energy-storage applications, Chem. Eur. J. 20 (2014) 13838–13852.
[8] S. Mao, G. Lu, J. Chen, Three-dimensional graphene-based composites for energy applications, Nanoscale 7 (2015) 6924–6943.
[9] K.S. Kim, Y. Zhao, H. Jang, S.Y. Lee, J.M. Kim, K.S. Kim, J.H. Ahn, P. Kim, J.Y. Choi, B. H. Hong, Large-scale pattern growth of graphene films for stretchable transparent electrodes, Nature 457 (2009) 706–710.
[10] Y. Zhu, S. Murali, W. Cai, X. Li, J.W. Suk, J.R. Potts, R.S. Ruoff, Graphene and graphene oxide: Synthesis, properties, and applications, Adv. Mater. 22 (2010) 3906–3924.
[11] C. Lee, X.D. Wei, J.W. Kysar, J. Hone, Measurement of the elastic properties and intrinsic strength of monolayer graphene, Science 321 (2008) 385–388.
[12] Y. Hernandez, V. Nicolosi, M. Lotya, F.M. Blighe, Z. Sun, S. De, I.T. McGovern, B. Holland, M. Byrne, Y.K. Gun'ko, J.J. Boland, P. Niraj, G. Duesberg, S. Krishnamurthy, R. Goodhue, J. Hutchison, V. Scardaci, A.C. Ferrari, J.N. Coleman, High-yield production of graphene by liquid-phase exfoliation of graphite, Nat. Nanotechnol. 3 (2008) 563–568.
[13] Y. Wu, B. Wang, Y. Ma, Y. Huang, N. Li, F. Zhang, Y. Chen, Efficient and large-scale synthesis of few-layered graphene using an arc-discharge method and conductivity studies of the resulting films, Nano Res. 3 (2010) 661–669.
[14] B.C. Brodie, On the atomic weight of graphite, Philosophical transactions of the Royal Society of London (1859) 249–259.
[15] W. Hummers, R. Offeman, Preparation of graphitic oxide, J. Am. Chem. Soc. 80 (1958) 1339–1339.
[16] T. Kuilla, S. Bhadra, D. Yao, N.H. Kim, S. Bose, J.H. Lee, Recent advances in graphene based polymer composites, Prog. Polym. Sci. 35 (2010) 1350–1375.
[17] S. Stankovich, D.A. Dikin, G.H.B. Dommett, K.M. Kohlhaas, E.J. Zimney, E.A. Stach, R.D. Piner, S.T. Nguyen, R.S. Ruoff, Graphene-based composite materials, Nature 442 (2006) 282–286.
[18] X. Huang, X. Qi, F. Boey, H. Zhang, Graphene-based composites 41 (2012) 666–686.
[19] M. Li, G. Sun, P. Yin, C. Ruan, K. Ai, Controlling the formation of rodlike V_2O_5 nanocrystals on reduced graphene oxide for high-performance supercapacitors, ACS Appl. Mater. Interfaces 5 (2013) 11462–11470.
[20] N.A. Kumar, H.J. Choi, Y.R. Shin, D.W. Chang, L. Dai, J.B. Baek, Polyaniline-grafted reduced graphene oxide for efficient electrochemical supercapacitors, ACS Nano 6 (2012) 1715–1723.
[21] X. Lu, H. Dou, B. Gao, C. Yuan, S. Yang, L. Hao, L. Shen, X. Zhang, A flexible graphene/multiwalled carbon nanotube film as a high performance electrode material for supercapacitors, Electrochim. Acta 56 (2011) 5115–5121.
[22] T. Lu, Y. Zhang, H. Li, L. Pan, Y. Li, Z. Sun, Electrochemical behaviors of graphene–ZnO and graphene–SnO_2 composite films for supercapacitors, Electrochim. Acta 55 (2010) 4170–4173.
[23] J. Yan, T. Wei, B. Shao, F. Ma, Z. Fan, M. Zhang, C. Zheng, Y. Shang, W. Qian, F. Wei, Electrochemical properties of graphene nanosheet/carbon black composites as electrodes for supercapacitors, Carbon 48 (2010) 1731–1737.
[24] Q. Cheng, J. Tang, J. Ma, H. Zhang, N. Shinya, L.C. Qinc, Graphene and carbon nanotube composite electrodes for supercapacitors with ultra-high energy density, Phys. Chem. Chem. Phys. 13 (2011) 17615–17624.
[25] H.J. Choi, S.M. Jung, J.M. Seo, D.W. Chang, L. Dai, J.B. Baek, Graphene for energy conversion and storage in fuel cells and supercapacitors, Nano Energy 1 (2012) 534–551.
[26] S. Chen, J. Zhu, X. Wu, Q. Han, X. Wang, Graphene oxide-MnO_2 nanocomposites for supercapacitors, ACS Nano 4 (2010) 2822–2830.
[27] R.B. Rakhi, W. Chen, D. Cha, H.N. Alshareef, High performance supercapacitors using metal oxide anchored graphene nanosheet electrodes, J. Mater. Chem. 21 (2011) 16197–16204.
[28] G. Wang, X. Shen, B. Wang, J. Yao, J. Park, Synthesis and characterisation of hydrophilic and organophilic graphene nanosheets, Carbon 47 (2009) 1359–1364.
[29] S. Park, J. An, J.R. Potts, A. Velamakanni, S. Murali, R.S. Ruoff, Hydrazine-reduction of graphite- and graphene oxide, Carbon 49 (2011) 3019–3023.
[30] S. Stankovich, D.A. Dikin, R.D. Piner, K.A. Kohlhaas, A. Kleinhammes, Y. Jia, Y. Wu, S.T. Nguyen, R.S. Ruoff, Synthesis of graphene-based nanosheets via chemical reduction of exfoliated graphite oxide, Carbon 45 (2007) 1558–1565.
[31] H.L. Poh, F. Sanek, A. Ambrosi, G. Zhao, Z. Sofer, M. Pumera, Graphenes prepared by Staudenmaier, Hofmann and Hummers methods with consequent thermal exfoliation exhibit very different electrochemical properties, Nanoscale 4 (2012) 3515–3522.
[32] D.D.L. Chung, Review: Exfoliation of graphite, J. Mater. Sci. 22 (1987) 4190–4198.
[33] S.R. Gajjela, K. Ananthanarayanan, C. Yap, M. Gratzel, P. Balaya, Synthesis of mesoporous titanium dioxide by soft template based approach: characterization and application in dye-sensitized solar cells, Energy Environ. Sci. 3 (2010) 838–845.
[34] G. Sun, X. Li, Y. Qu, X. Wang, H. Yan, Y. Zhang, Preparation and characterization of graphite nanosheets from detonation technique, Mater. Lett. 62 (2008) 703–706.
[35] A.C. Ferrari, J.C. Meyer, V. Scardaci, C. Casiraghi, M. Lazzeri, F. Mauri, S. Piscanec, D. Jiang, K.S. Novoselov, S. Roth, A.K. Geim, Raman spectrum of graphene and graphene layers, Phys. Rev. Lett. 97 (2006) 187401–187404.
[36] L.G. Cançado, A. Reina, J. Kong, M.S. Dresselhaus, Geometrical approach for the study of G′ band in the Raman spectrum of monolayer graphene, bilayer graphene, and bulk graphite, Phys. Review B 77 (2008) 245408.
[37] A. Kaniyoor, S. Ramaprabhu, A Raman spectroscopic investigation of graphite oxide derived graphene, AIP ADVANCES 2 (2012) 032183-1–032183-13.
[38] F. Bonhomme, J.C. Lasse'gues, L. Servant, Raman spectroelectrochemistry of a carbon supercapacitor, J. Electrochem. Soc. 148 (2001) E450–E458.